2009

Epitaxial growth of (001)-oriented Ba0.5Sr0.5TiO3 thin films on a-plane sapphire with an MgO/ZnO bridge layer

Bo Xiao
Virginia Commonwealth University, xiaob@vcu.edu

Hongrui Liu
Virginia Commonwealth University

Vitaliy Avrutin
Virginia Commonwealth University, vavrutin@vcu.edu

See next page for additional authors

Xiao, B., Liu, H., Avrutin, V., et al. Epitaxial growth of (001)-oriented Ba0.5Sr0.5TiO3 thin films on a-plane sapphire with an MgO/ZnO bridge layer. Applied Physics Letters, 95, 212901 (2009).

Epitaxial growth of (001)-oriented $Ba_{0.5}Sr_{0.5}TiO_3$ thin films on *a*-plane sapphire with an MgO/ZnO bridge layer

Bo Xiao,[1,a)] Hongrui Liu,[1] Vitaliy Avrutin,[1] Jacob H. Leach,[1] Emmanuel Rowe,[1] Huiyong Liu,[1] Ümit Özgür,[1] Hadis Morkoç,[1] W. Chang,[2] L. M. B. Alldredge,[2] S. W. Kirchoefer,[2] and J. M. Pond[2]

[1]*Department of Electrical and Computer Engineering, Virginia Commonwealth University, Richmond, Virginia 23284, USA*

[2]*Naval Research Laboratory Washington, Washington, DC 20375, USA*

(Received 7 September 2009; accepted 27 October 2009; published online 23 November 2009)

High quality (001)-oriented $Ba_{0.5}Sr_{0.5}TiO_3$ (BST) thin films have been grown on *a*-plane sapphire $(11\bar{2}0)$ by rf magnetron sputtering using a double bridge layer consisting of (0001)-oriented ZnO (50 nm) and (001)-oriented MgO (10 nm) prepared by plasma-assisted molecular beam epitaxy. X-ray diffraction revealed the formation of three sets of in-plane BST domains, offset from one another by 30°, which is consistent with the in-plane symmetry of the MgO layer observed by *in situ* reflective high electron energy diffraction. The in-plane epitaxial relationship of BST, MgO, and ZnO has been determined to be BST [110]//MgO [110]//ZnO $[11\bar{2}0]$ and BST [110]/MgO [110]// ZnO $[1\bar{1}00]$. Capacitance-voltage measurements performed on BST coplanar interdigitated capacitor structures revealed a high dielectric tunability of up to 84% at 1 MHz. © *2009 American Institute of Physics*. [doi:10.1063/1.3266862]

Ferroelectric materials have attracted much interest due to a unique combination of physical properties, which offer great promise for various applications.[1,2] The utilization of the strong dependence of dielectric permittivity on applied electric field in these materials has led to the realization of microwave passive components, such as tunable capacitors or varactors, phase shifters, modulators, etc.[3,4] The desire to achieve miniaturization of microwave components and systems is leading the development of thin-film-based microwave components. $Ba_xSr_{1-x}TiO_3$ (BST) thin films, being one of the most studied materials, have been extensively grown on a variety of substrates such as MgO, $LaAlO_3$, $SrTiO_3$, and sapphire.[5–8] Among these substrates, sapphire possesses advantages such as low cost, high chemical stability, and of particular importance, a low loss tangent which make sapphire an excellent substrate for passive microwave components.

Despite this motivation to use sapphire, growth of BST thin films on sapphire is not yet as established as on other substrates due in part to the difficulty in achieving high quality BST films. Large lattice mismatch and different crystal structures of BST and sapphire have apparently hampered the pace of this heterostructure growth. Polycrystalline BST films were generally reported on sapphire;[9,10] therefore, it is imperative to utilize a bridge layer (nucleation or seed layer) between BST and sapphire, which can accommodate the lattice mismatch and promote the crystallization of BST films for high structural perfection. For example, ultrathin (<1 nm) TiN layers have been introduced as bridge layers to grow (111)-oriented BST thin films on *c*-plane sapphire.[8] Here, we demonstrate the growth of high-quality (001)-oriented BST films on *a*-plane sapphire using a double MgO/ZnO bridge layer and report preliminary results of electrical measurements performed on interdigitated capacitor (IDC) structures. The choice of MgO buffer layer was dictated by a well-established BST growth on (001)-oriented MgO.[5] However, it is difficult to grow (001) MgO directly on sapphire because of a large lattice mismatch and dissimilar crystal structures. We found that the introduction of ZnO intermediate layer promotes the growth of (001)-oriented MgO. Additionally, doped ZnO layer can be utilized as a bottom electrode in parallel-plate capacitor structures.

MgO/ZnO bridge layers were grown epitaxially on *a*-plane sapphire by radio-frequency (rf) plasma-assisted molecular beam epitaxy (MBE). To achieve high quality ZnO films, a low-temperature ZnO buffer ~10 nm thick was first grown at a substrate temperature, T_S, of 300 °C followed by annealing at 700 °C. Next, a high-temperature ZnO layer was grown at T_S=550 °C. Both ZnO layers were grown at an oxygen pressure of 2×10^{-5} Torr. The MgO layer was grown at T_S=450 °C and an oxygen pressure of 9×10^{-6} Torr. The thicknesses of ZnO and MgO thin films were about 50 and 10 nm, respectively.

After the MgO/ZnO buffer layer was prepared, the substrate was immediately transferred into the rf magnetron sputtering chamber for BST growth. To avoid possible MgO decomposition, substrates with the MgO/ZnO layer were kept in oxygen ambient at 6 mTorr while the temperature was ramping up. The mixture of Ar [30 SCCM (SCCM denotes standard cubic centimeters per minute)] and O_2 (5 SCCM) were introduced into the growth chamber kept at 2 mTorr. The deposition rate was 450 Å/h at 120 W rf power and T_S=750 °C.

High-resolution x-ray diffraction (HRXRD) was employed to determine the structural properties of the thin films. As seen from Fig. 1, the 2θ-ω scan of HRXRD shows the reflections from the films of ZnO, MgO, and BST. The ZnO layer shows the (0002) reflection at 34.47°. Although the MgO layer is thin (10 nm), a weak diffraction peak consistent with the (002) MgO reflection can be seen at 42.93° in Fig. 1. Only the (00*l*) reflections from BST thin films are

a)Electronic mail: xiaob@vcu.edu.

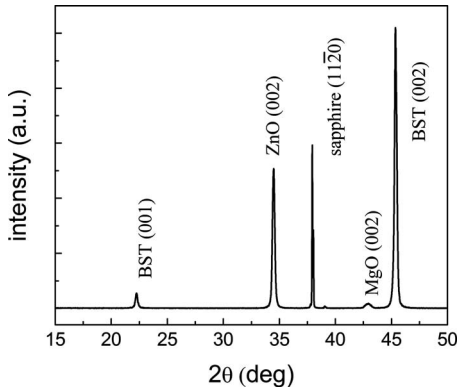

FIG. 1. 2θ-ω scan of the epitaxial BST/MgO/ZnO film on *a*-plane sapphire substrate.

observed. The absence of other reflections indicates that the [001] axes of BST films are well aligned with [0001] ZnO. The full width at half maximum (FWHM) of the BST (001) rocking curve is around 0.5° for the 300-nm-thick BST film. The out-of-plane lattice parameter *c* of BST was determined as 3.993 Å, which is larger than that of bulk BST.[11] The in-plane lattice parameter was ~3.91 Å from asymmetric BST (011) XRD reflections indicating that the films are under in-plane compressive strain. Similar structural parameters have been reported for BST on MgO substrates, where the large lattice parameters were correlated with the oxygen pressure during growth, and presumably due to the oxygen vacancies.[5,12,13] In addition, these factors such as lattice mismatch, difference of thermal expansion coefficients, and oxygen vacancies may act in unison to cause such lattice expansion.[7]

The growth progression of MgO/ZnO was monitored by *in situ* reflection high- energy electron diffraction (RHEED). As illustrated in Figs. 2(a) and 2(b), the streaky patterns along the [11$\bar{2}$0] and [1$\bar{1}$00] azimuths of ZnO revealed the two-dimensional growth mode of the ZnO film. The MgO film exhibits the same RHEED pattern along both azimuthal directions of ZnO in Figs. 2(c) and 2(d); that is, the pattern repeated itself every 30° of substrate rotation. These patterns are consistent with those taken along the [110] azimuthal directions of (001)-oriented MgO films.[14] A pattern characteristic of the [100] azimuth of MgO appears to be rotated by

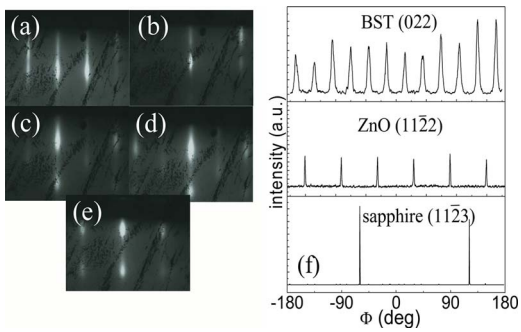

FIG. 2. (Color online) [(a)–(e)] RHEED patterns of MgO and ZnO grown on *a*-plane sapphire: (a) ZnO [11$\bar{2}$0] azimuth, (b) ZnO [1$\bar{1}$00] azimuth, (c) MgO parallel to ZnO [11$\bar{2}$0] azimuth, (d) MgO parallel to ZnO [1$\bar{1}$00] azimuth, and (e) MgO rotated by 15° with respect to ZnO [1$\bar{1}$00] and [11$\bar{2}$0] azimuths. (f) Φ scan patterns of asymmetrical reflections of BST (022), ZnO (11$\bar{2}$2), and *a*-sapphire (11$\bar{2}$3).

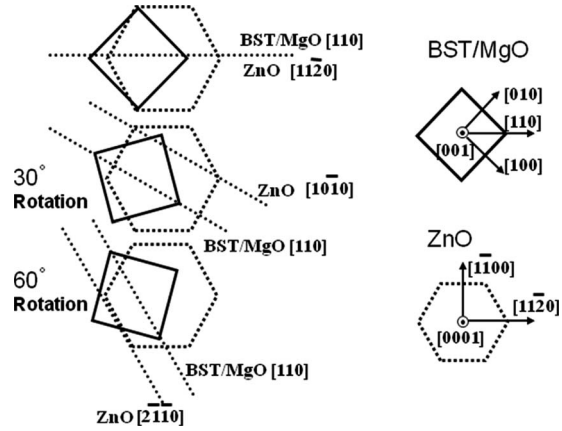

FIG. 3. In-plane epitaxial relationship between BST/MgO (001) and ZnO (0001).

15° from the [110] direction [Fig. 2(e)]. The observed behavior is inconsistent with the cubic symmetry of MgO and most likely points to the formation of three sets of 30° domains of (001) MgO. The results suggest the in-plane epitaxial relationship to be MgO [110]//ZnO [11$\bar{2}$0] and MgO [110]//ZnO [1$\bar{1}$00] due to domain structures.

To further examine the epitaxial relationships, Φ scans of XRD asymmetric reflections were performed. Φ scans of the (10$\bar{1}$2) and (11$\bar{2}$2) ZnO reflections and the (10$\bar{1}$3) and (11$\bar{2}$3) sapphire reflections indicated that the in-plane epitaxial relationships for ZnO on *a*-plane sapphire are ZnO [11$\bar{2}$0]//*a*-sapphire [0001] and ZnO [1$\bar{1}$00]//*a*-sapphire [1$\bar{1}$00], which are consistent with previous reports.[15,16] Figure 2(f) shows the Φ scans of BST (022), ZnO (11$\bar{2}$2), and sapphire (11$\bar{2}$3) reflections. The Φ scan of the BST (022) planes showed twelve reflection peaks rotated by 30° with respect to each other, which indicates the existence of three sets of BST domains. The results suggest the in-plane relationship of BST and ZnO to be BST [110]//ZnO [11$\bar{2}$0] and BST [110]//ZnO [1$\bar{1}$00]. Although XRD is not able to detect the asymmetric diffraction from the MgO film due to its thinness (10 nm), the above-mentioned results of RHEED indicate the same in-plane epitaxial relationships for the MgO layer on ZnO as those found for BST from XRD. Thus, it suggests that the BST film follows the in-plane alignment of the MgO on ZnO template, and the in-plane epitaxial relationships for the BST film and the MgO/ZnO layer are BST [110]//MgO [110]//ZnO [11$\bar{2}$0] and BST [110]//MgO [110]//ZnO [1$\bar{1}$00].

Figure 3 displays the possible in-plane alignments of BST and MgO lattices on ZnO. The in-plane projection of the ZnO unit cell is represented by the hexagons (dashed lines), and the projection of BST or MgO are the squares shown by solid lines. When BST/MgO lattice is not rotated with respect to the ZnO (upper left image) or rotated by 60°, one of the ⟨110⟩ directions of BST/MgO is parallel to ZnO ⟨11$\bar{2}$0⟩ (dotted lines in Fig. 3). For the case in which the BST/MgO is rotated by 30° with respect to ZnO, the same direction of BST/MgO is parallel to ZnO [10$\bar{1}$0]. This proposed relationship is consistent with our observation that the [100] direction of BST/MgO is rotated by 15° with respect to

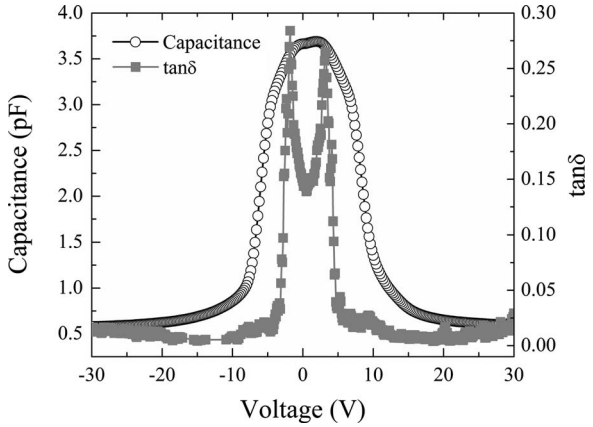

FIG. 4. Capacitance and loss tangent of BST/MgO/ZnO/*a*-sapphire capacitor structure.

the $\langle 11\bar{2}0\rangle$ direction of ZnO (or 15° rotation of BST/MgO (011) with respect to ZnO ($11\bar{2}2$)). This is confirmed by the results presented in the Φ scans of Fig. 2.

IDCs were fabricated on the BST films, which have a total of ten fingers with a finger width of 5 μm, a gap of 5 μm, and an aperture length of 75 μm. Capacitance-voltage (*C-V*) measurements were performed using a Hewlett-Packard 4284 *LCR* meter at 1 MHz. The voltage applied was swept from −30 to 30 V. In Fig. 4, the BST thin film on *a*-sapphire exhibits the maximum capacitance of 3.67 pF around zero bias and a minimum of 0.57 pF at 30 V that translates into a dielectric tunability of about 84% using the expression: $T=(C_{\max}-C_{\min})/C_{\max}[\%]$. Dissipation factor, loss tangent (tan δ), was also measured as a function of bias (Fig. 4). At the bias voltage larger than 5 V, the dissipation factor is ~0.007–0.02. It increases to 0.27 at ~4 V and then drops to 0.15 gradually as the bias approaches zero. This change in dissipation factor is most likely caused by the contribution of the ZnO layer. We expected the maximum dissipation factor to occur at zero electric field as both the BST and the ZnO layers would exhibit the most loss at low fields (due to free carriers responding to the high frequency signal). At high fields, the thin ZnO layer would be depleted, and thus its conductivity and dissipation factor should be at a minimum. However, when one considers the distribution of the electric field, it is noted that at the lowest field, the field penetrated into the ZnO is also at a minimum since the dielectric constant of BST is at its maximum. Therefore, the contribution of ZnO to the dissipation is lowest at low fields. As the field increases and dielectric constant of BST decreases, the penetration of the field into the ZnO increases and its contribution to loss is enhanced. We believe that this interplay between relative contributions of dissipation factor as a function of applied electric field accounts for the shape of the dissipation factor curve. Further investigation is needed to improve the quality of the ZnO buffer layer and lower the loss.

In conclusion, highly (001)-oriented BST thin films on *a*-plane sapphire have been achieved by rf sputtering with MBE-grown MgO/ZnO bridge layers. Based on the results of XRD measurements, the in-plane epitaxial relationships were found to be BST [110]/MgO [110]//ZnO [$11\bar{2}0$] and BST [110]/MgO [110]//ZnO [$1\bar{1}00$]. The in-plane alignment of BST on ZnO was predetermined by the MgO thin layer. High dielectric tunability of 84% found from *C-V* measurements on a coplanar capacitor structures is indicative of high quality BST thin films on *a*-plane sapphire.

This work is funded by the Office of Naval Research under the directions of Dr. I. Mack and Dr. D. Green.

[1]N. Setter, D. Damjanovic, L. Eng, G. Fox, S. Gevorgian, S. Hong, A. Kingon, H. Kohlstedt, N. Y. Park, G. B. Stephenson, I. Stolitchnov, A. K. Taganstev, D. V. Taylor, T. Yamada, and S. Streiffer, J. Appl. Phys. **100**, 051606 (2006).
[2]N. Izyumskaya, Ya. Alivov, S.-J. Cho, H. Morkoc, H. Lee, and Y.-S. Kang, Crit. Rev. Solid State Mater. Sci. **32**, 111 (2007).
[3]M. J. Lancaster, J. Powell, and A. Porch, Supercond. Sci. Technol. **11**, 1323 (1998).
[4]A. K. Tagantsev, V. O.Sherman, K. F. Astafiev, J. Venkatesh, and N. Setter, J. Electroceram. **11**, 5 (2003).
[5]L. M. B. Alldredge, W. Chang, S. B. Qadri, S. W. Kirchoefer, and J. M. Pond, Appl. Phys. Lett. **90**, 212901 (2007).
[6]C. M. Carlson, T. V. Rivkin, P. A. Parilla, J. D. Perkins, D. S. Ginley, A. B. Kozyrev, V. N. Oshadchy, and A. S. Pavlov, Appl. Phys. Lett. **76**, 1920 (2000).
[7]B. Xiao, V. Avrutin, H. R. Liu, E. Rowe, J. Leach, X. Gu, Ü. Özgür, and H. Morkoç, Appl. Phys. Lett. **95**, 010927 (2009).
[8]T. Yamada, P. Muralt, V. O. Sherman, C. S. Sandu, and N. Setter, Appl. Phys. Lett. **90**, 142911 (2007).
[9]E. A. Fardin, A. S. Holland, K. Ghorbani, E. K. Akdogan, W. K. Simon, A. Safari, and J. Y. Wang, Appl. Phys. Lett. **89**, 182907 (2006).
[10]D. Rafaja, J. Kub, D. Šimek, J. Lindner, and J. Petzelt, Thin Solid Films **422**, 8 (2002).
[11]JCPDS-ICDD Reference Code 00–039–1395.
[12]W. Chang, J. S. Horwitz, A. C. Carter, J. M. Pond, S. W. Kirchoefer, C. M. Gilmore, and D. B. Chrisey, Appl. Phys. Lett. **74**, 1033 (1999).
[13]L. M. Alldredge, W. Chang, S. W. Kirchoefer, and J. M. Pond, Appl. Phys. Lett. **94**, 052904 (2009).
[14]H. Yang, H. Al-Brithen, A. R. Smith, J. A. Borchers, R. L. Cappelletti, and M. D. Vaudin, Appl. Phys. Lett. **78**, 3860 (2001).
[15]J. B. Baxter and E. S. Aydil, J. Cryst. Growth **274**, 407 (2005).
[16]S.-H. Lim, D. Shindo, H.-B. Kang, and K. Nakamura, J. Cryst. Growth **225**, 202 (2001).